Desalination and Water Treatment
www.deswater.com
doi: 10.5004/dwt.2023.29459

290 (2023) 255–265
April

Application of motion simulation in fuzzy control of marine water plant protection robot

Shangzheng Liu*, Bin Liu

Nanyang Institute of Technology, School of Electronic and Electrical Engineering, Nanyang 473004, China, email: liushangzheng@mjc-edu.cn (S. Liu)

Received 18 April 2022; Accepted 10 July 2022

ABSTRACT

In order to overcome the problems of low control accuracy and long response time in traditional motion control methods of marine plant protection robot, this paper mainly studies the application of motion simulation in fuzzy control of marine plant protection robot. Firstly, the object motion simulation description algorithm of tree convex polyhedron is used to construct the working environment model of marine plant protection robot, and the marine plants are located by the model. Then, according to the positioning results, the motion equation of the marine plant protection robot is determined, and finally the fuzzy control of the marine plant protection robot is carried out. The experimental results show that, compared with the traditional method, this method has high control accuracy (up to 87%), short response time (up to 8.1 s), high signal strength, strong anti-interference ability and good application effect. It can be further popularized and applied.

Keywords: Motion simulation; Marine plant protection robot; Fuzzy control; Motion angle; Motion path

1. Introduction

Due to a large number of reclamation and aquaculture activities, the marine natural ecological environment is seriously damaged. Some important economic fish, shrimp, crab and shellfish habitats have disappeared, and many rare and endangered wild animals and plants have disappeared. This has greatly reduced the ability of the beach wetland to regulate climate, store water, resist storm surges, and protect land [1,2].

Due to long-term reclamation and felling, the degradation of many coastal mangroves has led to the disappearance of some valuable tree species, and a sharp decrease in the number of fish, shrimp, crabs, shellfish and the number of migratory birds in the forest [3]. The number of coral reefs in the sea is rapidly reduced due to the over exploitation of their medical and economic value of lime burning, and their rich communities are also destroyed [4]. The serious consequences will be that the beach's ability to withstand typhoons and storm surges will be reduced, further leading to coastal retreat, tree collapse and other disasters [5–8].

In recent decades, with the large-scale march to the sea, the marine ecological environment has been damaged more and more seriously, and marine natural disasters will be more difficult to control [9,10]. The deterioration of the marine environment makes people realize the importance of protecting the marine ecological environment. Therefore, the protection of marine plants has become an urgent problem in the process of modern economic development.

At this stage, robot has become one of the important symbols of scientific and technological achievements, and has been widely used in all walks of life [11]. There are many kinds of robots, including industrial robots, home robots, underwater robots and entertainment robots, etc. [12,13]. Among them, the marine plant protection robot has become the focus of research in related fields due to its special working properties.

* Corresponding author.

Li et al. [14] put forward a path tracking control method of mobile robot based on PID control. This method reconstructed the modules of mobile robot, and can quickly collect, extract and store the transmission signals of the main control module. At the same time, the method of PID was used to establish the accurate mathematical model for fuzzy control of mobile robot. Although it can complete the control, it is easy to be disturbed in the complex underwater environment and cannot effectively avoid collision. Lin et al. [15] proposed a three-dimensional simultaneous positioning and control method for autonomous mobile robot based on VSLAM. According to the position and pose state of the robot and the relevant data of the underwater environment, the method established the point cloud map of the working environment, and carried out the motion control of the autonomous mobile robot according to the map. The control operation is more sensitive. However, this method has low control accuracy and is not suitable for practical application. Braginsky and Guterman [16] proposed a control method of underwater vehicle equipped with forward-looking sonar. This method collected the working environment data in horizontal and vertical directions in real time. According to the collected results, the forward looking sonar equipment was used to provide the robot with obstacle information, and the robot motion control instructions were issued according to the information. This method can provide more accurate obstacle information, but the control effect of the robot is not ideal because the control accuracy parameters of the robot are not set effectively. Guerra et al. [17] proposed a disturbance compensation method based on dynamics standard and constructed a supervisory control framework which was used to adjust the robot's position and posture state, so as to control the robot's movement stability in a limited time. Although this method can control the robot, it does not analyze the complex working environment and lacks comprehensiveness.

In view of the disadvantages of the traditional methods, a fuzzy control method of marine plant protection robot based on motion simulation is proposed on the premise of fully considering wave and other factors. The experimental results show that the method can realize the autonomous and accurate control of the marine plant protection robot [18], provide an accurate solution to marine ecological problems, and provide reliable and effective technical references for future marine protection projects. The research steps are as follows:

- Step 1: The working environment model of the marine plant protection robot is built by using the target motion simulation description algorithm based on the tree shaped convex polyhedron;
- Step 2: According to the working environment model, the positioning of marine plants is completed;
- Step 3: Motion planning of the marine plant protection robot is carried out and its motion equation is determined, so as to reduce the deviation of motion path analysis and improve the control accuracy;
- Step 4: Fuzzy control is carried out on the marine plant protection robot. It is finally realized through fuzzy input, construction of language control rules and defuzzification of output.
- Step 5: Fuzzy control test experiment and result analysis;
- Step 6: Summary.

The research block diagram of this paper is shown in Fig. 1.

Through the above steps, this research is completed to solve the problems of low control accuracy and long response time of traditional motion control methods of plant protection robots.

This study can effectively avoid the destruction of marine living resources in the process of marine development, realize the rational utilization of marine resources, and ensure that the habitats and living places of marine animals and plants are not damaged, which has made outstanding contributions to the protection and development of marine resources. Besides, this study can also safeguard national sovereignty and territorial integrity, ensure the independence of national resources and the stability of people's lives, and is of great significance to the sustainable and healthy development of countries and regions.

2. Working environment modeling based on tree convex polyhedron

The complexity of the marine environment is much higher than land environments and others. The complexity

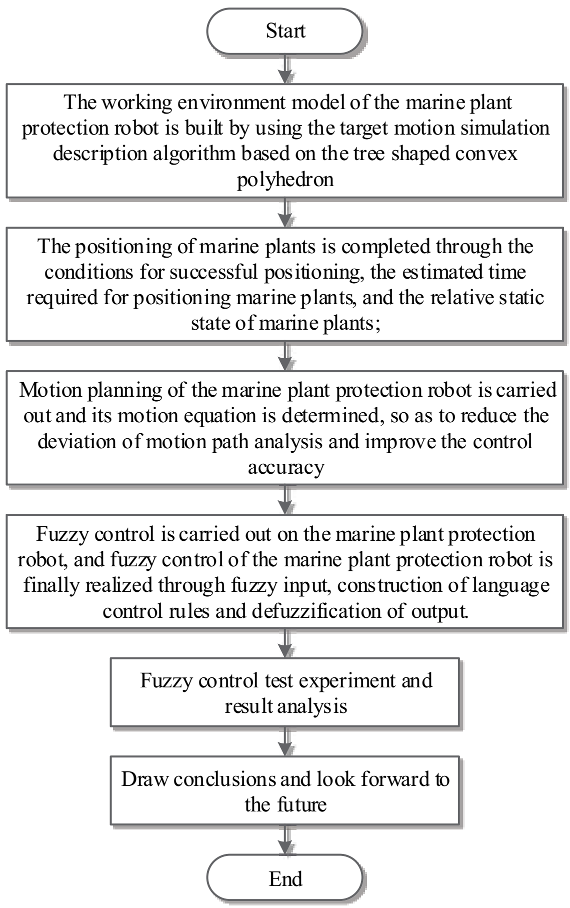

Fig. 1. Research block diagram of this paper.

of underwater environment is especially high, so it is necessary to focus on the analysis of the underwater environment [19–21]. The examples of underwater operation and onshore operation environment are shown in Figs. 2 and 3.

Based on the above analysis, the paper introduces the object motion simulation description algorithm based on tree convex polyhedron to model the working environment of the marine plant protection robot, and accurately locate the marine plants according to the model [22–24].

2.1. Construction of work environment model

The object motion simulation description algorithm of tree convex polyhedron is simply to construct a simulation environment by three elements: point, face and edge. The following two requirements should be met when using this method to model the work environment: First, a tree structure surrounded by tight polyhedron is established; Second, a fixed data structure is used to manage the model.

Under the influence of wave, gravity, buoyancy and other factors, assuming that the working environment has three symmetrical planes, then the model of the working environment can be described by Formula (1):

$$A = \begin{cases} \dfrac{\mathrm{Mv} + P_v(v)v + Q(v)v + G}{Z_{\max}} & \text{if underwater operation} \\ \dfrac{\mathrm{MKv} + P(k)_k + r}{Z_{\max}} & \text{if land operation} \end{cases} \tag{1}$$

Fig. 2. Example of underwater operation environment.

Fig. 3. Example of onshore operation environment.

The working environment is classified as underwater working environment and onshore working environment [25]. In the formula, v is used to describe the flow velocity; M is used to describe the inertia mass; $P_v(v)$ is used to describe the underwater temperature field; $Q(v)$ is used to describe the viscous hydrodynamic matrix; G is used to describe the static forces such as the gravity and buoyancy in the water; $Z_{\max}$ is used to describe the maximum dynamic force required for the movement of the objects in the water. K is the land operation area, $P_k(k)$ is the land temperature field and r is the wind force matrix.

According to the above formula, the real-time situation of the working environment can be analyzed, and the marine plants will be located according to the model.

2.2. Positioning of marine plants

There are many factors involved in the accurate positioning of marine plants [26,27]. When positioning the underwater marine plants, the judgment and positioning are mainly based on the differences in the appearance of the unit pixel. Assuming that the image appearance collected is significantly different from the image monitored by the monitoring equipment [28], the judgment of the marine plants can be made in the following forms:

- There is enough information in the image, and it can distinguish the underwater environment from the land environment;
- The information of marine plants is roughly located in the shortest time to be extracted. [29,30];
- Based on the working environment model, the location of marine plants is carried out [31].

In conclusion, the conditions for the successful positioning of marine plants are summarized as follows:

$$\max(T_i, T_w) < T \tag{2}$$

where w is used to describe the mobile range of marine plant protection robot [32], T is used to describe the total searching time of marine plants, and T_i is used to describe the estimated time required to locate marine plants. T is calculated by:

$$T = \frac{n}{V} \tag{3}$$

where V is used to describe the displacement speed of marine plants affected by factors such as resistance and buoyancy during positioning, and n is used to describe the relative static state of marine plants.

The calculation formula of n is:

$$n \begin{cases} \dfrac{v}{a}, a \neq 0 \\ \infty, a = 0 \end{cases} \tag{4}$$

where a is used to describe the acceleration of the movement of marine plants.

On the basis of positioning underwater marine plants, it is necessary to analyze the motion path of the marine plant protection robot.

3. Robot motion planning

The marine plant protection robot belongs to a kind of strong nonlinear system, which means that all freedom motions are coupled with others, and the coupling details cannot be effectively described in qualitative form [33]. Besides, the marine plant protection robot mainly runs in uncertain and complex environment, therefore, it needs to be reasonably and effectively controlled to ensure that it can complete its tasks quickly, accurately and safely [14].

3.1. Selection of spatial coordinate system

Assuming that the whole underwater vehicle is a rigid body with constant mass and volume, the essence of its motion control is the general motion of the rigid body under the action of gravity and hydrodynamic forces in the fluid. Establish two coordinate systems: fixed coordinate system and moving coordinate system. Each coordinate determines the corresponding orientation according to the right-hand rule, so the underwater operation environment is shown in Fig. 4.

The fixed coordinate system (E–ξηξ) is also known as the inertial coordinate system, or "fixed system" for short. The origin E is any point on the earth, and the $E\xi$ axis is in the positive direction with the main heading of the robot; The $E\eta$ axis is perpendicular to the $E\zeta$ axis, that is, 90° to the $E\xi$ axis according to the right-hand rule; The $E\zeta$ axis is always perpendicular to the coordinate plane $\xi E\eta$, and points to the center of the earth in a positive direction; The motion coordinate system (O–xyz) is also known as the carrier coordinate system, or "moving system" for short. The origin O is generally located at the center of gravity of the robot, with the Ox axis pointing to the bow of the robot, the Oy axis pointing to the starboard, and the Oz axis pointing to the bottom of the robot. The motion parameters and motion coordinate components on the motion coordinate system are shown in Table 1.

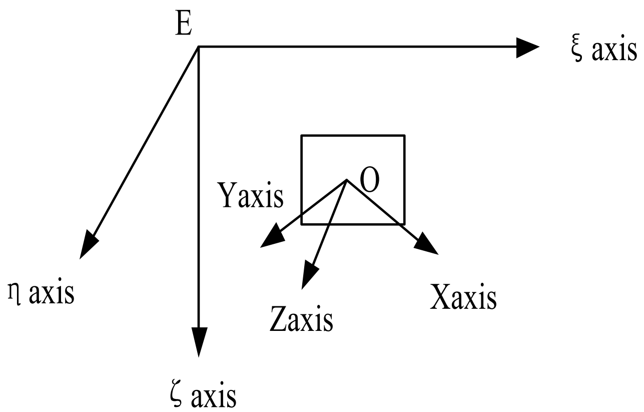

Fig. 4. Diagram of fixed coordinate system and moving coordinate system.

3.2. Spatial motion equation

Through the above, conditions are provided for the positioning of marine plants, and after the positioning of marine plants, the motion equation of the robot can be determined to ensure more accurate positioning of marine plants [34].

The underwater motion of the robot is essentially a six degree of freedom spatial motion, which can be achieved by moving the robot along three axes.

The translational motion of the three axes and the rotational motion around them are respectively represented.

3.2.1. Translational motion equation

According to Newton's second theorem, the expression of the force on the underwater robot is as follows:

$$m\frac{dV_G}{dt} = F_g \tag{5}$$

where m represents the quality of the robot; V_G represents the velocity of the center of gravity.

In order to meet the generality of the motion of the underwater robots, the velocity V_G of the center of gravity can be divided into the following two items:

$$V_G = V + D \times R_G \tag{6}$$

where V represents the speed of the origin of the dynamic system in the fixed system; D represents the rotational angular velocity of the power train. $D = d/a_r$, where d is used to describe the difference between the desired velocity vector direction angle and the current velocity vector direction angle; a_r is used to describe the rotational angular acceleration of the dynamic system; R_G represents the distance from the center of gravity to the coordinate origin; $D \times R_G$ indicates implicated speed.

The vector expression of the center of gravity acceleration V_G is as follows:

$$\hat{V}_G = \frac{dV_G}{dt} = \frac{d\left(V + D \times R_G\right)}{dt} = \hat{V} + D \times R_G + a_r \times \left(D \times R_G\right) \tag{7}$$

where $\hat{V}$ represents the acceleration of the lower origin of the dynamic system.

By substituting the velocity of the origin of the dynamic system in the fixed system, the acceleration of the origin of the dynamic system, the rotational angular velocity of the dynamic system, the rotational angular acceleration of

Table 1
Motion parameters and motion coordinate components

Vector	X-axis	Y-axis	Z-axis
Speed V	u	v	w
Angular velocity D	p	q	r
Power F_g	X	Y	Z
Moment M_o	K	M	N

the dynamic system, the center of gravity coordinates, and the force received by the robot, namely $V=\begin{pmatrix}u & v & w\end{pmatrix}^T$, $\hat{V}=\begin{pmatrix}\hat{u} & \hat{v} & \hat{w}\end{pmatrix}^T$, $D=\begin{pmatrix}p & q & r\end{pmatrix}^T$, $a_r=\begin{pmatrix}\hat{p} & \hat{q} & \hat{r}\end{pmatrix}^T$, $R_G=\begin{pmatrix}x_G & y_G & z_G\end{pmatrix}^T$, $F_g=\begin{pmatrix}X & Y & Z\end{pmatrix}^T$ into Formula (7), the expressions of the three components of the dynamic system, namely, the translational motion equation, can be obtained:

$$\begin{cases} X=m\left[\hat{u}-vr+wq-x_G\left(q^2+r^2\right)+y_G\left(pq-\hat{r}\right)+z_G\left(pr+\hat{q}\right)\right] \\ Y=m\left[\hat{v}-wp+ur-y_G\left(r^2+p^2\right)+z_G\left(qr-\hat{p}\right)+x_G\left(qp+\hat{r}\right)\right] \\ Z=m\left[\hat{w}-uq+vp-z_G\left(p^2+q^2\right)+x_G\left(rp-\hat{q}\right)+y_G\left(rq+\hat{p}\right)\right] \end{cases} \quad (8)$$

3.2.2. Rotational motion equation

The relationship between the relative momentum moment of the underwater robot to the origin o of the moving system and the torque received can be obtained from the relative momentum moment of the moving point of the particle system. The specific relationship is as follows:

$$\frac{dH'_o}{dt}=M_o+R_G\times\left(-m\hat{V}\right) \quad (9)$$

where H'_o represents the relative momentum moment of the particle system calculated by the relative velocity to the origin o of the moving system; M_o represents the external torque at the origin o of the power train.

According to the definition of relative moment of momentum $H'_o = I_o\Omega$, I_o is the moment of inertia of the robot relative to the origin O of the dynamic system in each coordinate axis:

$$I_o=\begin{bmatrix} I_x & -I_{xy} & -I_{xz} \\ -I_{yx} & I_y & -I_{yz} \\ -I_{zx} & -I_{zy} & I_z \end{bmatrix} \quad (10)$$

Since the robot is roughly symmetrical in structure about the xOz and xOy planes, therefore:

$$I_o=\begin{bmatrix} I_x & 0 & 0 \\ 0 & I_y & 0 \\ 0 & 0 & I_z \end{bmatrix} \quad (11)$$

Substituting $\hat{V}=\frac{dV}{dt}$ and $H'_o = I_o\Omega$ into the Formula (9) yields:

$$\frac{dI_o\Omega}{dt}=M_o-R_G\times m\frac{dV}{dt} \quad (12)$$

From the derivative relationship of vectors in fixed and dynamic systems:

$$I_oa_r+D\times\left(I_oD\right)=M_o-R_G\times\left(\hat{V}+D\times V\right) \quad (13)$$

By substituting $D=\begin{pmatrix}p & q & r\end{pmatrix}^T$, $R_G=\begin{pmatrix}x_G & y_G & z_G\end{pmatrix}^T$, $V=\begin{pmatrix}u & v & w\end{pmatrix}^T$, $\hat{V}=\begin{pmatrix}\hat{u} & \hat{v} & \hat{w}\end{pmatrix}^T$ into Formula (13), the rotational motion equations of the three coordinate axes of the underwater vehicle can be obtained:

$$\begin{cases} K=I_x\hat{p}+\left(I_z-I_y\right)qr+m\left[y_G\left(\hat{w}+vp-uq\right)-z_G\left(\hat{v}+ur-wp\right)\right] \\ M=I_y\hat{q}+\left(I_x-I_z\right)rp+m\left[z_G\left(\hat{u}+wq-vr\right)-x_G\left(\hat{w}+vp-uq\right)\right] \\ N=I_z\hat{r}+\left(I_y-I_x\right)pq+m\left[x_G\left(\hat{v}+ur-wp\right)-y_G\left(\hat{u}+wq-vr\right)\right] \end{cases} \quad (14)$$

Targeting at ensuring the safety of the robot, the space motion equation of the robot is determined, which reduces the deviation of motion path analysis and improves the control accuracy [35].

4. Fuzzy control of marine plant protection robot

After positioning the marine plants, the control of the marine plant protection robot is realized by fuzzy processing of the input and constructing language control rules [36].

The control design of the marine plant protection robot mainly includes three stages: fuzzy processing of the input, construction of language control rules, and real output, namely, defuzzy processing of the output [37,38].

4.1. Fuzzification of input quantity

The fields of input x and output y are described by sets X and Y in turn. According to the detailed requirements of robot function, the fuzzy control [39] selects the position deviation Δl and the speed deviation Δl as the input x, which are [–0.5 m, 0.5 m] and [–0.1 m/s, 0.1 m/s], respectively. The control quantity $y(t)$ represents the control output amount to the marine plant protection robot.

In essence, fuzzy processing is to obtain the corresponding language variables of input x in the domain. In order to facilitate analysis, it is necessary to discretize the domain, that is to say, complete the normalization of input domain. In this section, the domain interval is set as [–6, 6], and the fuzzy control [40] input quantity is discretized to this range. If the domain of input quantity x is (a,b), then it can be converted to the change quantity x' of [–6, 6] interval by the following formula:

$$x'=\frac{12}{b-a}\left(x-\frac{a+b}{2}\right) \quad (15)$$

Membership function is the application basis of fuzzy control. Typical membership functions include trapezoidal membership function, triangular membership function, Gaussian membership function and generalized bell membership function. Triangular membership functions are composed of straight lines, which can accurately distinguish each language variable and ensure the correctness of fuzzy control logic. The distribution diagram of linguistic variable values is drawn by trigonometric membership function, as shown in Fig. 5. After the fuzzy processing, the set of input and output fuzzy variables can be expressed as {NL, NM, NS, ZO, PS, PM, PB}.

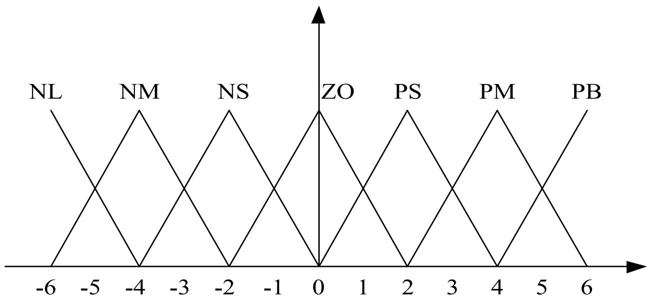

Fig. 5. Example of distribution of language variable values in robot operating environment.

4.2. Construction of language control rules

The motion state of the marine plant protection robot is analyzed. When the position deviation Δl and velocity deviation Δv of the robot are both negative large (NL), the robot deviates from the target motion state. To adjust the motion of the robot and make it closer to the target, the control amount needs to be adjusted to be positive large (PL) [41]. When the robot position deviation Δl is negative large (NL) and the velocity deviation Δv is positive large (PL), the robot and the target state are far from each other, but they are more and more similar to the robot target state. When the control amount is changed into positive small (PS), that is to say, only a small amount of adjustment is needed to make the marine plant protection robot move according to the given state and track.

4.3. Defuzzification of output

Fuzzy rules are the core of the whole fuzzy logic control link. The number of rules is related to the division of fuzzy subsets of fuzzy variables. The finer the division is, the more rules are. However, it does not mean that the higher the accuracy of the rule base is. The finer the division is, the longer the running time of the fuzzy controller will be. There are multiple motion modes for marine plant protection robot, and fuzzy rules are required to cover all working conditions. The fuzzy control rules of marine plant protection robot are based on the understanding of the physical characteristics of the controlled object and the intuition and experience of control. With the expert experience as a reference, and in combination with the control objectives and operation mode of the marine plant protection robot's fuzzy control, multiple fuzzy rules are formulated to carry out relevant fuzzy reasoning.

The result cannot be directly regarded as a control quantity, which is mainly because it is a fuzzy result, so it needs to be defuzzied to turn it into an accurate value that can be realized by the execution unit [42]. The main purpose of defuzzification is to calculate the fuzzy conclusion by fuzzy reasoning, which can reflect the accurate distribution of control quantity. At present, there are many defuzzification methods. In this section, the center of gravity method, also known as the center of mass method, is the most reasonable method among all defuzzification methods. The formula is described as follows:

$$y_0 = \frac{\int_y^k \mu(y) y dy}{\int_y^k \mu(y) dy} \tag{16}$$

In the formula, the integral symbol ∫ represents the algebraic integral of the membership value of all elements of the output fuzzy subset in the continuous domain μ. y represents the influence degree of the anti-fuzzy output, and d represents the membership degree of the fuzzy subset. If the membership function of fuzzy subset is discrete domain, its calculation formula is:

$$y_0 = \frac{\sum_{i=1}^{n} \mu(y_i) y_i}{\sum_{i=1}^{n} \mu(y_i)} \tag{17}$$

where i represents the central value of the maximum membership.

The working environment of the marine plant protection robot is very complex. If the marine plant protection robot encounters the marine plant when it is moving, the corresponding control strategies are obtained according to different situations, and the marine plant protection robot achieves the best control effect.

Based on the above positioning of marine plants and the motion planning of marine plant protection robots, the motion prediction and accurate control can be realized in advance, and finally the fuzzy control of marine plant protection robots can be realized.

5. Experimental results and analysis

In order to verify the validity of the fuzzy control method of marine plant protection robot based on motion simulation, a comparative experiment is carried out. The experimental environment is Dell PC. The processor is Intel core-m480i5cpu @ 2.67GHz, with 4GB memory. The operating system is 32-bit windows7 system, and the simulation experimental data are all from MATLAB software. Dolphins have vigorous and flexible physiological characteristics, and mainly rely on echo location function during activities. Dolphin robot is a kind of bionic robot for dolphins. It has a streamlined shell of dolphins and can locate through sonar in underwater environment. It has the advantages of low noise, simple control and high mobility. It can basically meet the requirements of underwater exploration. Existing researchers have used the bionic dolphin robot to explore dangerous waters, so this experiment chooses the dolphin robot as the experimental object. The submergence depth of the robot is 150 m, and the speed is 0–1 m/s. The robot is loaded with a detachable mechanical arm. The size of the submersible is 690 mm × 410 mm × 100 mm. All the above data are from a robot manufacturer who produces the robot according to strict parameter standards. The application process of this study is shown in Fig. 6.

In the experiment, the method in reference [43], the method in reference [44] and the proposed method are

(a)
(b)
(c)

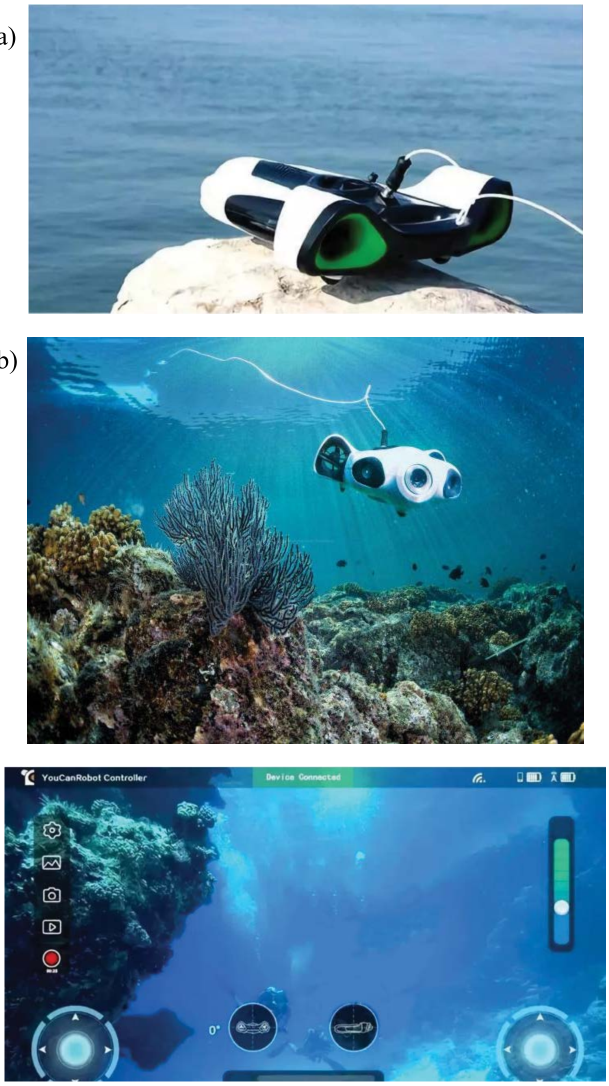

Fig. 6. The application process of this study.

compared and analyzed under the conditions with interference and without interference, respectively [43] described the problem of a group of marine robots measuring underwater environmental parameters in local areas. The centralized control method of robot group work plan was adopted to design the centralized control system of marine robots, so as to control autonomous underwater robots and autonomous surface vehicles, and relevant results were obtained. The centralized control equation of the ocean robot is as follows:

$$P=\begin{cases}P_1=\left(p^{(1)}_{\text{АНПА}},p^{(1)}_{\text{АНВА}}\right)\\P_2=\left(p^{(2)}_{\text{АНПА}},p^{(1)}_{\text{АНВА}}\right)\\P_3=\left(p^{(3)}_{\text{АНПА}},p^{(1)}_{\text{АНВА}}\right)\\\ldots\\P_n=\left(p^{(n)}_{\text{АНПА}},p^{(n)}_{\text{АНВА}}\right)\end{cases} \tag{18}$$

In Eq. (18), $\left(p^{(1)}_{\text{АНПА}},p^{(2)}_{\text{АНПА}},p^{(3)}_{\text{АНПА}},\ldots,p^{(n)}_{\text{АНПА}}\right)$ represents the angular velocity parameter in the process of robot movement, and $\left(p^{(1)}_{\text{АНВА}},p^{(2)}_{\text{АНВА}},p^{(3)}_{\text{АНВА}},\ldots,p^{(n)}_{\text{АНВА}}\right)$ represents the linear velocity parameter in the process of robot movement.

Alam et al. [44] was mainly based on the hexapod robot model with buoyancy model as force interference, and combines the derived impedance control based on the center of mass (COM) with fuzzy logic control to control it, so as to reduce the influence of underwater buoyancy on the control of hexapod motion state.

The derived impedance is used to control the robot drive motor, and the derived impedance control equation is as follows:

$$z=\frac{Z_L}{Z_O}=\frac{\left(R+jX\right)}{Z_O}=r+jX \tag{19}$$

In Eq. (19), Z_L represents equivalent resistance, Z_o represents equivalent reactance, R represents impedance loss coefficient, j represents impedance angle, r represents impedance mode, and X represents load impedance parameters.

Fuzzy logic is used to control the motion attitude and direction of the robot. The specific control equations are as follows:

$$\begin{cases}y^1=c_0^1+c_1^1x_1+c_2^1x_2+\ldots+c_n^1x_n\\y^2=c_0^2+c_1^2x_1+c_2^2x_2+\ldots+c_n^2x_n\\\ldots\\y^N=c_0^N+c_1^Nx_1+c_2^Nx_2+\ldots+c_n^Nx_n\end{cases} \tag{20}$$

In Eq. (20), x_1, x_2, …, x_n represents fuzzy rules, c_0^1, c_1^1, …, c_n^1 represents fuzzy sets 1, c_0^2, c_1^2, c_2^2, …, c_n^2 represents fuzzy sets 2, c_0^N, c_1^N, c_2^N, …, c_n^N represents fuzzy sets N, and y^1, y^2, …, y^N represents different fuzzy controllers.

Because the method in reference [43] and the method in reference [44] are the same as the proposed method in the method design, taking into account the robot's own weight, control cable length, power and power parameters, etc., the fairness and consistency of the comparative experiment can be guaranteed [45]. Taking control accuracy and response time as experimental indexes, the effectiveness of the proposed method is analyzed.

5.1. Anti-interference test

5.1.1. Without interference

During the experiment, the test samples are input into the simulation software for trial operation to test the software operation. When the software operation status is normal, the test samples are input into the simulation software for experiment. In the process of simulation experiment, set no signal interference, and import the data packets of different methods to the simulation platform to drive the relevant programs of the simulation experiment, so as to obtain the experimental results of obstacle avoidance accuracy without interference.

Fig. 7 is a comparison of the accuracy of controlling the underwater obstacles by using the methods of reference [43], reference [44] and the proposed method without interference.

It can be seen from the analysis of Fig. 7 that, without being affected by external conditions, the obstacle avoidance accuracy of the marine plant protection robot in the [43] varies from 60% to 70%, the obstacle avoidance accuracy of the marine plant protection robot in the [44] method varies from 58% to 80%, while the obstacle avoidance accuracy of the marine plant protection robot in this method always varies from 80% to 90%, indicating that only this method can accurately control the obstacle avoidance of the marine plant protection robot, The proposed method has significant advantages.

5.1.2. Under interference condition

In the simulation experiment process, the current interference and current interference parameters are introduced, and the data package execution programs of different methods are imported to the simulation platform to drive the relevant programs of the simulation experiment, and the experimental results of obstacle avoidance accuracy under interference conditions are obtained.

When marine plant protection robots work in a complex underwater environment, they are disturbed by various factors, such as wind, waves and current. Therefore, whether the proposed method can effectively control the marine plant protection robot under the interference of the external environment needs to be tested. Fig. 8 is a comparison diagram of control accuracy between the methods in reference [43], reference [44] and the proposed method under the interference of current and wave.

It can be seen from the analysis of Fig. 8 that under the condition of ocean current interference and wave interference, the control accuracy of the method in reference [43] is up to 30% and kept below 30% all the time; The control accuracy of the method in reference [44] is higher than that of the method in reference [43], and the highest is 60%; However, there is still a big gap between the two methods and the proposed method, and the control accuracy of the proposed method is kept above 65%, and the highest is 87%. It shows that the fuzzy control method of the marine plant protection robot can reduce the influence of the interference factors and realize the precise control of the marine plant protection robot [46].

5.2. Signal strength comparison

In order to further verify the anti-interference ability of different methods, the signal strength comparison test is conducted. During the experiment, the test samples are input into the simulation software for trial operation to test the software operation. When the software operation status is normal, the test samples are input into the simulation software for experiment. In the process of simulation experiment, set the signal interference intensity to 60 dB, import the data package of different methods' execution program to the simulation platform, drive the relevant programs of simulation experiment, calculate and analyze the output signal strength of different methods, and obtain the signal strength comparison results under different sample data, as shown in Fig. 9.

It can be seen from the analysis of Fig. 9 that the maximum signal strength of the method in method in reference [43] is 58 dB, and the maximum signal strength of the method in reference [44] is 73 dB. However, the signal under the control of this method is sparse, indicating that there is a signal data loss. Compared with the other two methods, the signal strength of the method in this paper is up to 73 dB, and the signal is relatively dense, which shows that the signal data under the control of this method is not easy to lose, and that this method has strong anti-interference ability.

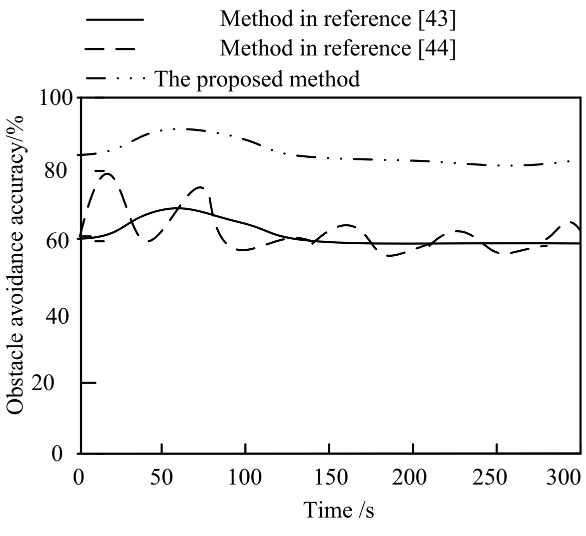

Fig. 7. Comparison results of obstacle avoidance accuracy of different methods without interference.

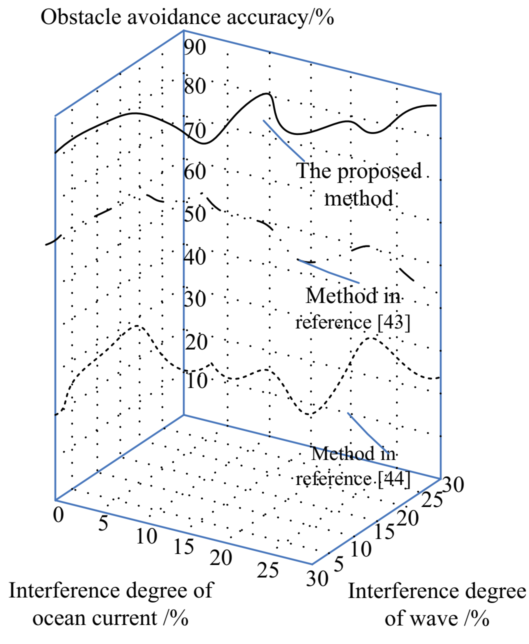

Fig. 8. Comparison results of control accuracy of different methods under interference conditions.

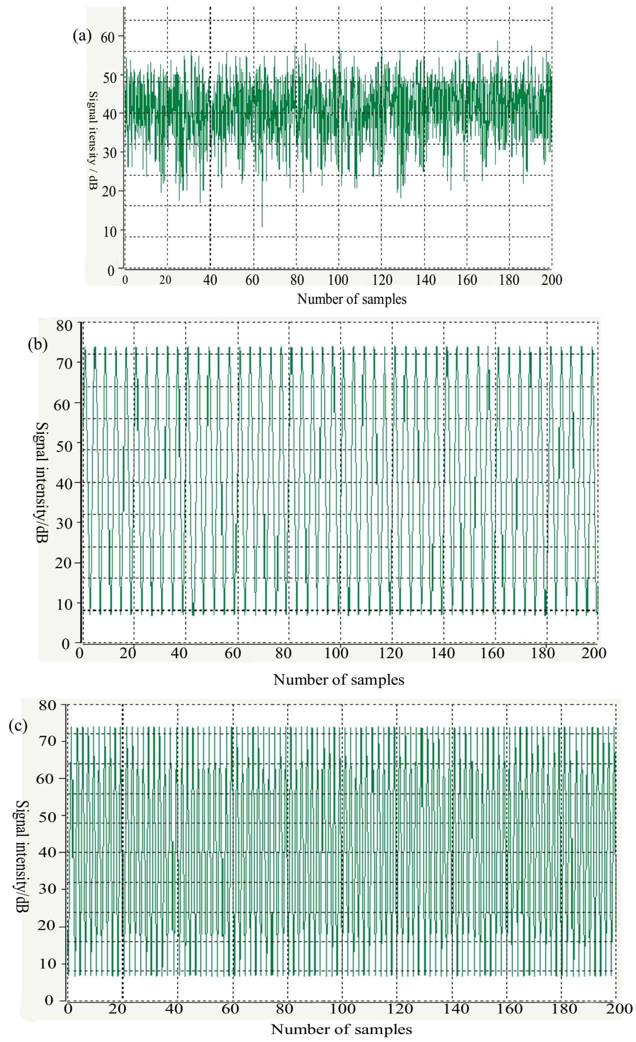

Fig. 9. Signal strength results of three different methods.

5.3. Response time comparison

The response time of the methods in reference [43], reference [44] and the proposed method are compared and analyzed, and the results are shown in Table 2.

The data in Table 2 shows that the response time of the reference method [43] is 19.1 s at the fastest and 31.22 s at the slowest; The response time of the reference method [44] is 19.1s at the fastest and 37.1 s at the slowest; The reaction time of the proposed method is 8.1 s at the fastest and 11.6 s at the slowest. The proposed method is significantly lower than that of the two traditional methods, which further verifies the high efficiency of the proposed method. The marine plant protection robot can respond to commands in time and improve the control efficiency.

To sum up, the control results obtained by the proposed method indicates that it can effectively achieve the control of underwater robot under the interference of wave and other external environment. Although there is a certain degree of vibration, the vibration amplitude is small, the control accuracy is high, and the response time is short, which can meet the needs of practical engineering.

Table 2
Response time of three methods

Method	First response time (s)	Second response time (s)	Third response time (s)	Fourth response time (s)
The proposed method	11.6	8.1	9.6	9.02
Method in Reference [43]	19.1	25.1	31.22	28.2
Method in Reference [44]	19.1	25.2	26.4	37.1

6. Conclusion

At present, the marine environment is constantly being infringed. If the ocean is polluted, human beings will also be in danger. It is necessary to protect the ocean because protecting the ocean means protecting human life! Therefore, the whole world should make joint efforts and take practical measures to protect and preserve the marine environment on which mankind depends. The application of marine plant protection robot is the main way to solve the above problems. The marine plant protection robot belongs to a complex nonlinear system, which needs to be controlled by a reasonable control method to ensure the stability and accuracy of the robot in the process of performing tasks. Therefore, a new fuzzy control method of marine plant protection robot based on motion simulation is proposed, which mainly constructs the working environment model of marine plant protection robot by using the target motion simulation description algorithm of tree convex polyhedron, and then locates marine plants according to the modeling results. Then, according to the positioning results, the motion equation of the marine plant protection robot is determined, and finally the fuzzy control of the marine plant protection robot is carried out. The experimental results show that, under the interference of external environment such as waves, this method can also effectively achieve the accurate control of marine plant protection robots, with the control accuracy maintained at more than 65%, and the highest accuracy is 87%, indicating strong anti-interference ability. It also shows short response time. The shortest time is only 11.6 s. It is hoped that this research can be popularized and provide certain application value for the protection of marine environment in the future, we should protect the marine environment on which human beings rely for survival in a more comprehensive way. In the future, it is necessary to apply the marine plant protection robot to the marine development and protection work, and use the method in this paper to carry out fuzzy control on the marine plant protection robot, so as to effectively avoid the collision between the robot and obstacles during the task execution, better perform the marine protection task, and promote the protective development of marine resources. In order to further expand the application scope of this method, it is necessary to apply this method to other robot fuzzy control fields for relevant application exploration, in order to promote the further development of robot control technology.

Data availability statement

The datasets used and/or analyzed during the current study are available from the corresponding author on reasonable request.

Conflicts of interest

The authors declare that there is no conflict of interest regarding the publication of this paper.

Funding statement

This work was supported by the Project of Fundamental and Frontier Science of Henan Province, Research of Intelligent Infrared and Visible Image Adaptive Fusion System (No. 162300410194).

References

[1] J. Ryu, K.-b. Liu, T.A. Bianchette, T. McCloskey, Identifying forcing agents of environmental change and ecological response on the Mississippi River Delta, Southeastern Louisiana, Sci. Total Environ., 794 (2021) 148730, doi: 10.1016/j.scitotenv.2021.148730.
[2] Y. Wang, H. Wang, B. Zhou, H. Fu, Multi-dimensional prediction method based on Bi-LSTMC for ship roll, Ocean Eng., 242 (2021) 110106, doi: 10.1016/j.oceaneng.2021.110106.
[3] J. Adounkpe, C. Agboton, W.A. Hounkpatin, B. Kounouhewa, C. Ahouannou, B. Sinsin, Qualitative assessment of table salt production techniques in southern Benin republic, and related mangrove destruction and health issues, Food Nutr. Sci., 12 (2021) 759–773.
[4] M.O. Amfa, M.I. Abdurrahman, S.A. Hidayat, G.L. Situmeang, F.K. Yudha, Macrobenthos community structure in coral reef ecosystem around Pramuka Island, Jakarta, IOP Conf. Ser.: Earth Environ. Sci, 420 (2020) 012003, doi: 10.1088/1755-1315/420/1/012003.
[5] G. Wang, Marine disaster prediction based on mathematical model, J. Coastal Res., 107 (2020) 230–245.
[6] T.X. Hoang, D.T. Le, H.M. Nguyen, N. Vuong, Labor market impacts and responses: the economic consequences of a marine environmental disaster, J. Dev. Econ., 147 (2020) 1–10.
[7] W. Zheng, X. Liu, L. Yin, Research on image classification method based on improved multi-scale relational network, PeerJ Comput. Sci., 7 (2021a) e613, doi: 10.7717/peerj-cs.613.
[8] Z. Ma, W. Zheng, X. Chen, L. Yin, Joint embedding VQA model based on dynamic word vector, PeerJ Comput. Sci., 7 (2021) e353, doi: 10.7717/peerj-cs.353.
[9] Y. Cao, K.D. Yin, X.M. Li, Prediction of direct economic loss caused by marine disasters based on the improved GM (1,1) model, J. Grey Syst., 23 (2020) 1–10.
[10] W. Zheng, X. Liu, L. Yin, Sentence representation method based on multi-layer semantic network, Appl. Sci., 11 (2021b) 1316–1329.
[11] F. Ghanipoor, A. Alasty, H. Salarieh, M. Hashemi, M. Shahbazi, Model identification of a marine robot in presence of IMU-DVL misalignment using TUKF, Ocean Eng., 206 (2020) 107344, doi: 10.1016/j.oceaneng.2020.107344.
[12] Z. Yan, B. Ouyang, D. Li, H.L. Liu, Y.N. Wang, Network intelligence empowered industrial robot control in the F-RAN environment, IEEE Wireless Commun., 27 (2020) 58–64.
[13] J. Wang, F. Liang, H. Zhou, M. Yang, Q. Wang, Analysis of position, pose and force decoupling characteristics of a 4-UPS/1-RPS parallel grinding robot, Symmetry, 14 (2022) 825, doi: 10.3390/sym14040825.
[14] Z.J. Li, C.G. Yang, C.Y. Su, Vision-based model predictive control for steering of a nonholonomic mobile robot, IEEE Trans. Control Syst. Technol., 24 (2016) 553–564.
[15] H.C. Lin, Q. Lv, G.S. Wang, Y. Zhang, B. Liang, 3D simultaneous localization and mapping for mobile robot based on VSLAM, J. Comput. Appl., 37 (2017) 2884–2887.
[16] B. Braginsky, H. Guterman, Obstacle avoidance approaches for autonomous underwater vehicle: simulation and experimental results, IEEE J. Oceanic Eng., 41 (2016) 882–892.
[17] M. Guerra, D. Efimov, Z. Gang, W. Perruquetti, Finite-time obstacle avoidance for unicycle-like robot subject to additive input disturbances, Auton. Robots, 41 (2017) 1–12.
[18] J. Lubinski, H. Olszewski, Hybrid finite element method development for offshore structures' calculation with the implementation of industry standards, Pol. Mar. Res., 26 (2019) 90–100.
[19] G. Vasiljevic, T. Petrovic, B. Arbanas, S. Bogdan, N. Kottege, Dynamic median consensus for marine multi-robot systems using acoustic communication, IEEE Rob. Autom. Lett., 5 (2020) 5299–5306.
[20] C. Xu, H. Xu, Self-tuning method of electronic governor parameters for marine medium-speed diesel engine, J. Coastal Res., 103 (2020) 378–381.
[21] W. Zheng, X. Liu, X. Ni, L. Yin, B. Yang, Improving visual reasoning through semantic representation, IEEE Access, 9 (2021c) 91476–91486.
[22] S. Li, X. Zhang, Z. Ding, The impact of public participation on the environmental impact assessment of marine engineering, J. Coastal Res., 103 (2020) 479–483.
[23] G. Liu, Data collection in mi-assisted wireless powered underground sensor networks: directions, recent advances, and challenges, IEEE Commun. Mag., 59 (2021) 132–138.
[24] B.M. Yilmaz, E. Tatlicioglu, A. Savran, M. Alci, Self-adjusting fuzzy logic based control of robot manipulators in task space, IEEE Trans. Ind. Electron., 69 (2022) 1620–1629.
[25] R. Xiao, H. Zhu, Y. Xue, H. Jiang, C. Chen, J. Zhu, Influence of the conical seamount on underwater sound propagation in a 3D shallow sea environment, J. Phys. Conf. Ser., 1592 (2020) 012019, doi: 10.1088/1742-6596/1592/1/012019.
[26] T. Liu, Y. Xiao, Y. Feng, J. Li, B. Huang, Guaranteed cost control for dynamic positioning of marine surface vessels with input saturation, Appl. Ocean Res., 116 (2021) 102868–102879.
[27] W. Zheng, L. Yin, X. Chen, Z. Ma, S. Liu, B. Yang, Knowledge base graph embedding module design for visual question answering model, Pattern Recognit., 120 (2021d) 108153–108163.
[28] M.H. Korayem, M. Yousefzadeh, S. Manteghi, Dynamics and input-output feedback linearization control of a wheeled mobile cable-driven parallel robot, Multibody Sys. Dyn., 40 (2016) 1–19.
[29] S. Sun, S. Qin, Y. Hao, G. Zhang, C. Zhao, Underwater acoustic localization of the black box based on generalized second-order time difference of arrival (GSTDOA), IEEE Trans. Geosci. Remote Sens., 59 (2020) 7245–7255.
[30] D. Li, S.S. Ge, T.H. Lee, Simultaneous-arrival-to-origin convergence: sliding-mode control through the norm-normalized sign function, IEEE Trans. Autom. Control, 37 (2021) 1966–1972.
[31] L. Zhang, C. Tang, P. Chen, Y. Zhang, Gaussian parameterized information aided distributed cooperative underwater positioning algorithm, IEEE Access, 8 (2020) 64634–64645.
[32] Y.N. Gusenitsa, O.A. Shiryamov, V.L. Rzhavitin, A.V. Khodak, A.M. Smirnov, Method for estimating underwater robot control parameters, IOP Conf. Ser.: Earth Environ. Sci., 872 (2021) 012004, doi: 10.1088/1755-1315/872/1/012004.
[33] J.J. Jiang, P.D. Franco, A. Alessandro, Shared control for the kinematic and dynamic models of a mobile robot, IEEE Trans. Control Syst. Technol., 24 (2016) 1–13.
[34] P.F. Huang, F. Zhang, X.D. Xu, Z.J. Meng, Z.X. Liu, Y.X. Hu, Coordinated coupling control of tethered space robot using releasing characteristics of space tether, Adv. Space Res., 57 (2016) 1528–1542.
[35] C.G. Yang, X.Y. Wang, L. Cheng, H.B. Ma, Neural-learning-based telerobot control with guaranteed performance, IEEE Trans. Cybern., 99 (2016) 1–12.
[36] P.G. José Manuel, M. Eduardo, S. Carlos, Distributed coverage estimation and control for multirobot persistent tasks, IEEE Trans. Rob., 32 (2016) 1444–1460.

[37] Z.J. Zhang, S.Y. Chen, S. Li, Compatible convex-nonconvex constrained QP-based dual neural networks for motion planning of redundant robot manipulators, IEEE Trans. Control Syst. Technol., 99 (2018) 1–9.
[38] F. Liu, G. Zhang, J. Lu, Multisource heterogeneous unsupervised domain adaptation via fuzzy-relation neural networks, IEEE Trans. Fuzzy Syst., 29 (2020) 3308–3322.
[39] Y. Sun, J. Xu, H. Qiang, W. Wang, G. Lin, Hopf bifurcation analysis of maglev vehicle-guideway interaction vibration system and stability control based on fuzzy adaptive theory, Comput. Ind., 108 (2019a) 197–209.
[40] Y. Sun, J. Xu, H. Qiang, G. Lin, Adaptive neural-fuzzy robust position control scheme for maglev train systems with experimental verification, IEEE Trans. Ind. Electron., 66 (2019b) 8589–8599.
[41] K. Melanie, H. Sandra, Invariance control for safe human-robot interaction in dynamic environments, IEEE Trans. Rob., 99 (2017) 1–16.
[42] S. Lounis, F. Matthieu, F. Antoine, 2D observer-based control of a vascular microrobot, IEEE Trans. Autom. Control, 62 (2017) 2194–2206.
[43] I. Tuphanov, A. Scherbatyuk, Some marine trial results of centralized control system for marine robot group, Ubs, 59 (2016) 233–246.
[44] M.M. Alam, A. Irawan, T.Y. Yin, Buoyancy effect control in multi legged robot locomotion on seabed using integrated impedance-fuzzy logic approach, Indian J. Mar. Sci., 44 (2015) 1937–1945.
[45] M. Medvedeva, T.E. Simos, C. Tsitouras, V. Katsikis, Direct estimation of SIR model parameters through second-order finite differences, Math. Methods Appl. Sci., 44 (2021) 3819–3826.
[46] B. Wang, F.C. Zou, J. Cheng, S.M. Zhong, Fault detection filter design for continuous-time nonlinear Markovian jump systems with mode-dependent delay and time-varying transition probabilities, Adv. Differ. Equations, 2017 (2017) 1–23.